Nonlinear Finite Element Analysis of Reinforced High Strength Concrete Corbels with and Without Steel Fiber and Shear Reinforcement

Assist.Prof.Dr. Aqeel H. Chkheiwer , Mustafa A. k. Essa

Abstract- This research presents a nonlinear finite element investigation on the behavior of high strength reinforced concrete corbels by using ANSYS program. A theoretical study using the finite element method is presented in the current work on fifty four corbels specimens divided into three series. Series one divides into two parts , The first part contained six specimens for comparing with the experimental results .The main parameters in this part are type of concrete (high strength concrete **HSC** and normal strength concrete **NSC**), compressive strength and shear span to effective depth ratio without steel fiber. while second part of series one contains six specimens and analyzes proposed specimen by finite element only to study other factors that were not discussed by the researcher in the first part. Series two, comprises fourteen reinforced high-strength concrete corbels, the main variables studied were concrete compressive strength, main reinforcement ratio(ρ_w), shear reinforcement stress ($\rho_h f y_h$), and the ratio of outside depth to the total depth of the corbel (*k/h*). Series three divides into two parts , The first part contained Seventeen high strength reinforced-concrete corbels for analytical of experimental result, where the main variables were (steel fiber content (V_f%), shear span-to-depth ratio (a/d), compressive strength concrete (f′c), main reinforcement ratio (ρ_w) and shear reinforcement stress ($\rho_h f y_h$). while second part contents eight specimens and analyzes proposed specimen by finite element only to study other factors that were not discussed by the researcher in the first part of series three.

The results show that the difference in the type of concrete (from **NSC** to **HSC**), increase the ultimate shear strength of the corbel specimens by about 17.9 and 25.4 % at a/d=0.6 and 20.2% and 35.5% at a/d=0.45
The increasing in horizontal reinforced index *ρh.fyh* was more active for corbels with *f´c*=60 MPa than corbels with *f´c*=40 or 50 MPa. When *k/h* increase from (0.24) to (1.00), the ultimate load increase by 12.3%.

A comparison with ACI318-M14 , Fatuhi's equation and Truss Model were conducted, the factor of safety against shear failure that can be obtained by using Truss Angle Method increase with increasing the concrete compressive strength, (a/d) value, and presence or absence horizontal stirrup. Truss Angle Method equation is mostly less conservative when compared with the ACI Code equation while Fatuhi's equation show increase ultimate shear strength when increase the fiber content. The values of ultimate shear strength that obtained by ACI-code less than experimental results.

Keywords— ANSYS, Shear Friction Method, High Strength Concrete (HSC), Normal Strength Concrete (NSC), corbels, Truss Angle Method, steel fiber.

u

1 Introduction

Brackets and corbels are short cantilevers having shear span depth ratio (*a/d)* they should not be greater than one percent tending to go as deep beams or simple trusses better than flexural members [1] . In recent years, the employment of HSC has raised quickly as a result of the request for high resistance, relatively lighter weight, and durable concrete. The main variance between the NSC and HSC is that the HSC trends to act as an elastic and more brittle material corresponded with NSC[2] . The observed inverse relationship between strength and ductility is a serious drawback if the employment of HSC is to be considered in some construction uses. However, such a impediment can be overcame through addition of height strength steel fibers. adding fibers to the brittle cement and concrete materials can offers a suitable particle and an economical way of predomination their ingrained disadvantage of poor tension and impact strength and enhances several of the construction characteristics characteristic of the primary material like fracture toughness, flexural resistance and strength to the effect of impact, thermal shock or spalling. Essentially, fiber behaves to crack arrest and restrict the growth of cracks , so the mixture turns into an ingrained fragile template[3]. Corbels (or brackets) which are single block built with columns (or walls), are usually used to support precast beams , slabs and any other form of precast structural system. In the last three decades several studies were made research the behavior of reinforced concrete corbels[4]. The choice of the panels or membrane elements was intended to isolate the effect of other unpreferred combination of stresses, and focus on the reduction of concrete.

2.Finite element analysis

Finite element method (FEM) is a theoretical way for analyzing a differentials or integrations equations and getting proximity solutions to a range variety of engineering problems. It has been applied to a number of physical problems, where the governing differential equations are available. The method essentially consists of assuming the continuous function for the solution and obtaining the parameters of the functions in a manner that

reduces the error in the solution. ANSYS is a general purpose software, used to simulate interactions of all disciplines of physics, structural, vibration, fluid dynamics, heat transfer and electromagnetic for engineers[5]. In this work, a three-dimensional finite element model by using ANSYS software computer program release 16.1has been made. Materials idealization and the elements used to build this model are listed below:

2.1 Element type

A Solid65 element is used to model the concrete. 1.2 A Link8 element is used to model steel reinforcement.

In the existing study the corbel is modeled using separate reinforcement. Therefore, a value of zero was inserted for all real constants that turned the smeared steel ability of the Solid 65 element off, except in case of representation of steel fiber as a smeared layer. In this work Material Number, was entered 5 (which refers steel fiber material number), and Volume Ratio as it is assumed (its value and orientation). The summation of the distribution ratios in x, y and z direction is equal to the main volume fraction of steel fiber in the matrix V_f=1% as shown in Table (1) .

Table (1) Real Constants representation for materials used in present study

Structural component	Finite element representation	Element designation in ANSYS
Concrete (SFRHSC)	8-node brick element (3 translation DOF pernode)	SOLID 65
Steel reinforcement bars	2-node discrete element (3 translation DOF per node)	LINK 180
Steel plates (at supports and load application)	8-node brick element (3 translation DOF per node)	SOLID 185

2.2 Material Properties

For convenience, the specimens were tested in an inverted position, therefore the specimens were modeled according to the laboratory as shown in Fig.(1). & Fig.(2) By making use of the symmetry of loading, geometry and reinforcement distribution of the tested corbels, only one half of the length will be considered in the numerical analyses. Responses of concrete under loading without and with confinement are characterized by distinctly nonlinear behaviors, which can be modeled in the SOLID65 element[6]. In this work the average concrete compressive strength values were between (33.75 to 106.5) MPa [7]. Poisson's ratio for concrete in all corbels is assumed to be 0.2. The shear transfer coefficient represents a shear strength reduction factor for subsequent loads that induce sliding (shear) across the crack face. The shear transfer coefficient ranges from 0.0 to 0.95 with 0.0 representing a smooth crack (complete loss of shear transfer) and 1.0 a rough crack (no loss of shear transfer). For an open crack, the shear transfer coefficient varied between 0.05 and 0.30 in many studies of reinforced concrete structures. Coefficient values selected (between 0 and 1) do not appear to be critical; however, a value greater than 0 is necessary to prevent numerical difficulties [6]. In order to model the steel reinforcement, Link 8 element is used .Where ANSYS define the steel reinforcement by two parts, the first one is linear elastic material model which defined by Elastic modulus (Es) and Poisson's ratio (ν). And the second part is bilinear inelastic to represent the stress-strain behavior of material which defined by two values the Yield stress (fy) and the Tangent modulus (Etan).

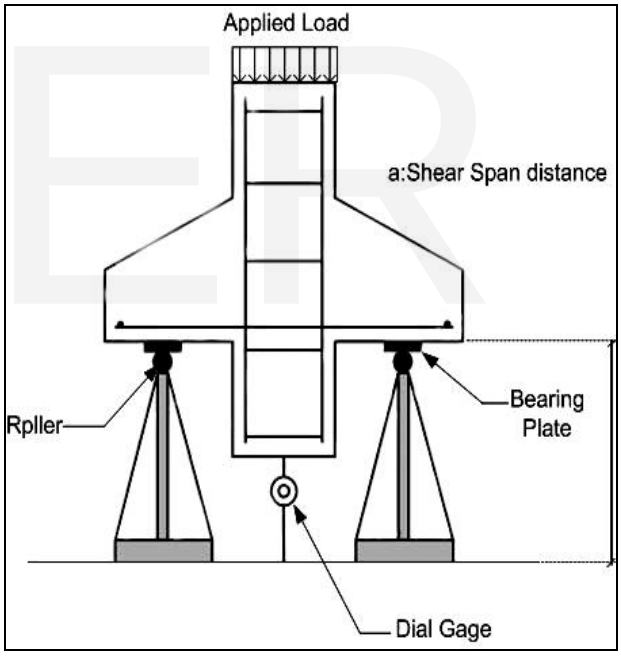

Fig .(1) Loading arrangement with Load Application measurement instrumentations on corbels

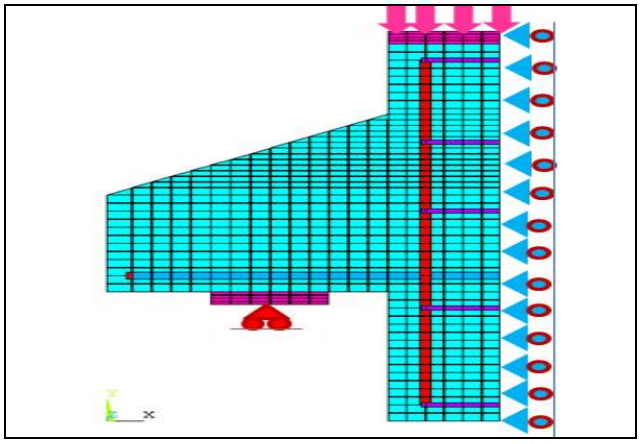

Fig (2) Representation of Specimens in ANSYS

3.Detail of study

The corbels investigated in this study are taken from three series.

The first series divided into two parts, The first part derived from (Mosleh et. al.) in (2014)[8].The basic purpose of this series study is to investigate the behaviour and strength of self-compacting reinforced concrete corbels. The number of specimens was tested 6 corbels subjected to vertical load where the clear depth to overall depth rates (a/d) where they were (0.3,0.45,0.6), and compressive strengths (f'c) of self-compacting concrete were varied .A corbel sketch with the main geometric properties is shown in Fig (3).The second part contains six models, was analyzed by Finite Element only to take some parameters that were not discussed by the researcher in the first series were discussed in this part such the effect of increasing the size of the column

The second series consist of first part that conducted on R.C corbel column members based on the past test investigated by Omar and Sedeeq .[9] The series consist of fourteen reinforced high-strength concrete corbels divided to five group were discussed the several parameter, including effect of difference compressive strength concrete (f'c), outside depth to the height of corbel rate (k/d), main tension reinforcement and horizontal shear reinforced.

The third series divided into two parts, The first part contained seventeen high strength, R.C corbels to verify the accuracy of the FEM by comparing with past test investigated carried out by (*Hafez et a)l*[10].In this part studied of "shear" behavior of high strength R.C corbels (with /without) fibers .The experimental parameters included volume of fiber fracture (V_f%), clear depth to overall depth rate a/d, compressive strength, primary tensile area and existence of shear reinforcement. The second part contains eight models, was analyzed by Finite Element only to take some parameters that were not discussed by the researcher in the first series were discussed in this part such increase the width of plate. The details of specimens Table (2).

Table (3) shows good agreement for the finite element solution compared with the experimental results throughout the entire range of behavior .They reveal that both the initial and post-cracking stiffness are reasonably predicted. The computed failure loads for all corbels are close to the corresponding experimental collapse load.

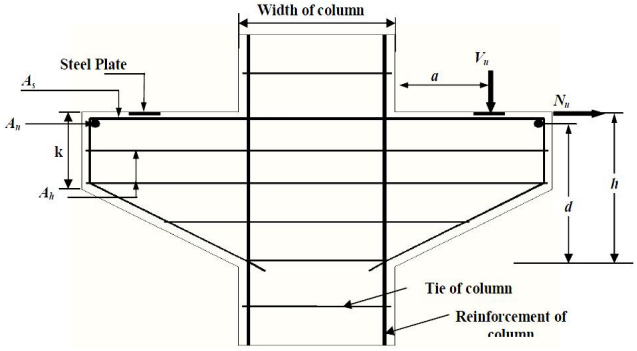

Fig. (3) Typical Reinforced Concrete Corbel

4.Parametric Studies

To study the influences of some of the material and solution factors on the nonlinear finite element analysis of high strength fiber concrete corbels. This study helps to clarify the effect of deference factors that have been considered on the maximum loads ,load-deflection and crack pattern for present numerical study with past experimental study which RC corbels model were analyzed by using ANSYS . The main variables included in this study were, concrete strength (*f´c*), clear depth to overall depth rate (*a/d*), primary steel area (A_s), present shear reinforcement , steel fibres content" (*Vf%*)and the outside to the total depth ratio (k/h)

4.1 Load Deflection relationship

The load deflection relationship from Finite Element and content a similarity with the experiment deflection outcomes for test samples that shows good agreement, but it was observed that there was a difference between the load deflection curve obtained by using ANSYS program when compared with the experimental load deflection curve. This difference occurred in two stages,

first stage, a stage before cracking, where the loads obtained from the experimental results were greater than ANSYS program due to percent some parameters which can reason this variation in results. Micro cracks are found in the concrete to some degree that can lower the stiffness of the real corbels, while the FEM don't include this parameter in consideration. In the FEM, perfect bond

between the concrete and steel reinforcing is supposed but, this presumption isn't real for the actual corbels.

second stage, after cracking, the load deflection curve of the loads obtained from the were greater ANSYS program than experimental results due to the macro crack can transfer stresses in RC corbel due to ,overlapping aggregates, effective screw and friction as below in (Fig 4a).When fibers are present, an increase in strength capacity and at the same time the ductility improved (Fig 4b). Rising the clear depth to overall depth rate (a/d) decreasing the failure load and increasing the deflection of corbels with and without fibers (Fig 5). As expected, increasing concrete strength causes to rise carrying capacity of the corbels. Also, it is noticed that the ductility of FRC corbels increased in comparison with those without fibers. This confirms the advantage of using fiber in increasing ductility of corbels (Fig 6). Increase the main steel ratio results in increasing corbel strength. Effect of addition of fibers to improve behaviour of specimen was clear in case of corbels having smaller main steel ratio (Fig 7). Using horizontal stirrups, gives a little increase in corbels strength and decreases deflection of corbels. Moreover, the addition of fibers allows the attainment of complete flexural capacity and, consequently, a more ductile response (Fig 8).

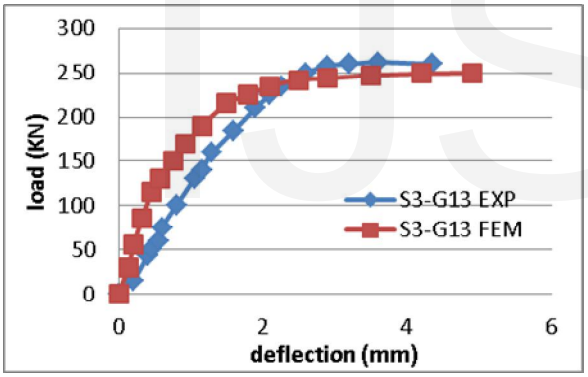

a) load deflection curve for S3-G13

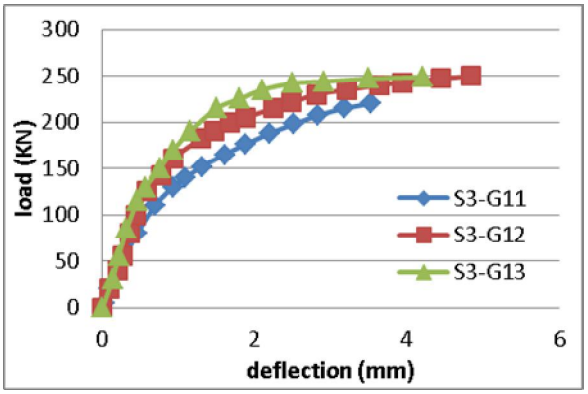

b) Influence of steel fibre content on load- deflection curve

Fig (4) Influence of fibre content on load-deflection curve

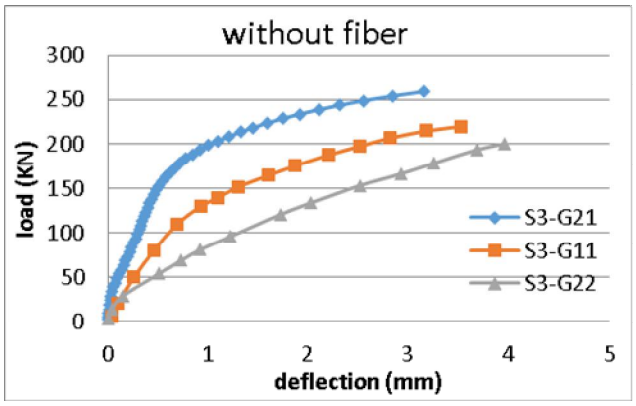

a) Without fiber

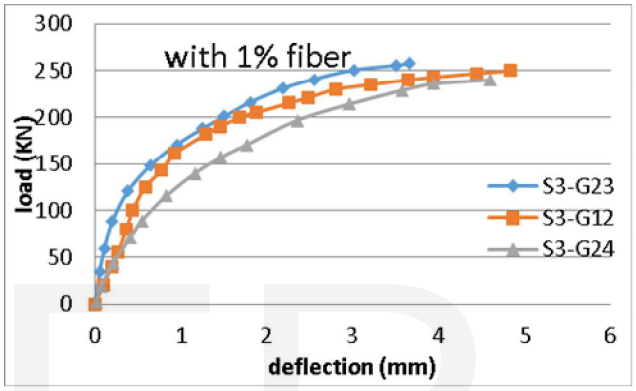

b) With 1% fiber

Fig (5) Influence of clear depth to overall depth on load-deflection curve

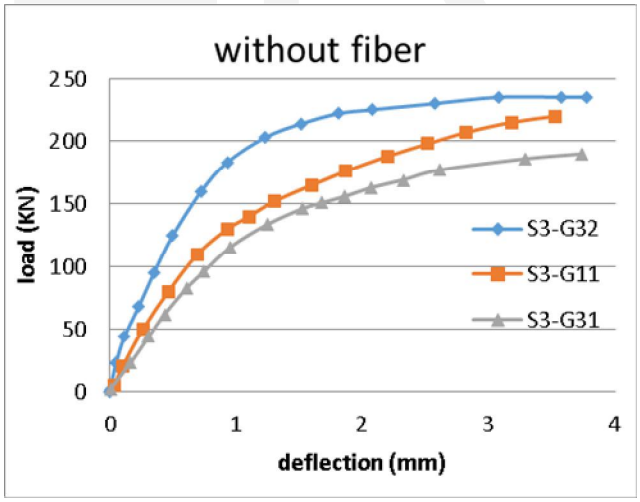

a) Without fiber

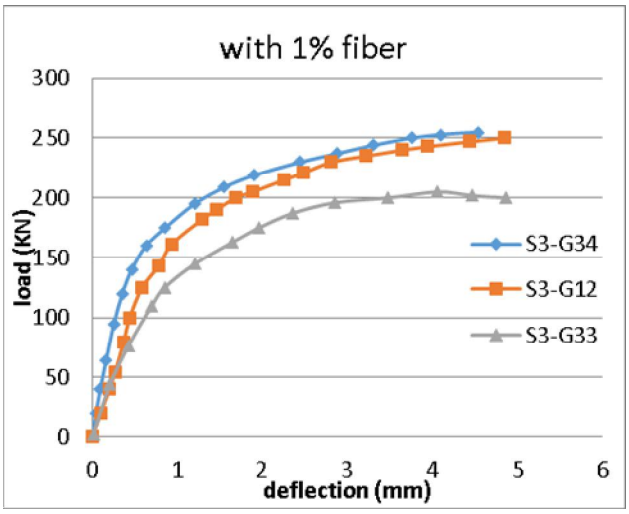

b) With fiber

Fig (6) Influence of concrete strength on load- deflection curve

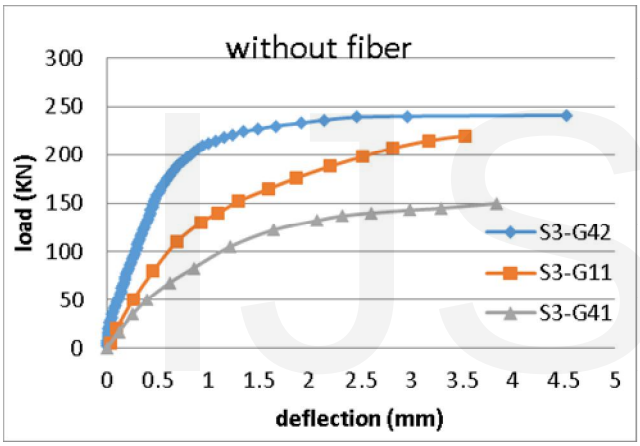

a) Without fiber

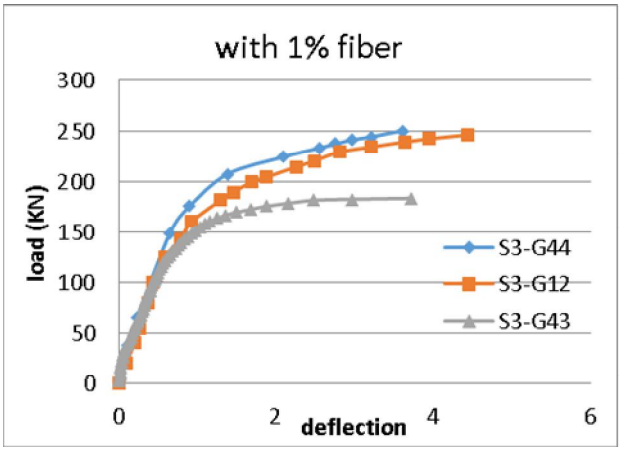

b) With 1% fiber

Fig 7 Effect of area of main reinforcement on load-deflection curve

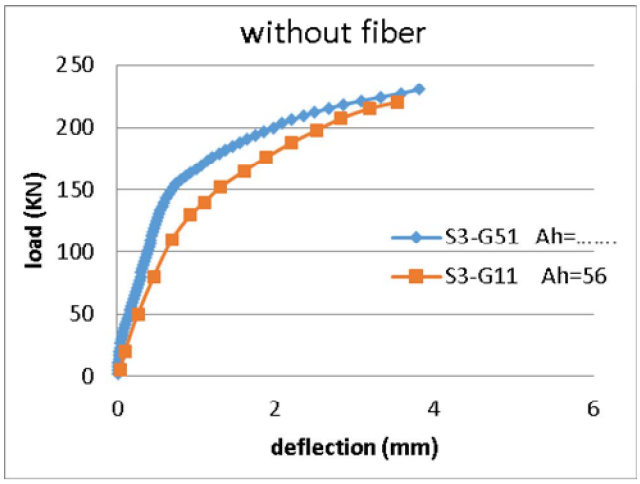

a) Without fiber

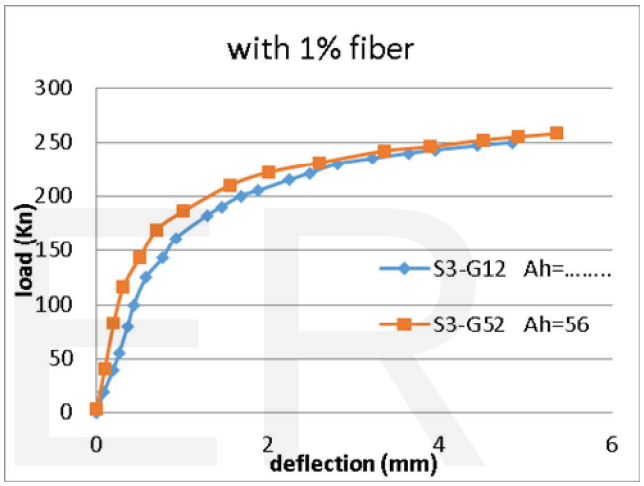

b) with 1% fiber

Fig (8) Effect of horizontal stirrups on load-deflection curve

5. Comparison with Test Results

5.1 Effect of Studied Variables on ultimate load and deflection

The obtained test results were analyzed to declare the influence of the deference factors included in this work on strength and deformation up to failure. These properties were measured by means of ultimate load and maximum deflection, as follows:

5.1.1 Effect of Steel Fiber Content:

Fig (9) shows that increase in fiber contents from 0% to 1.0% and 1.5% results in an increase in ultimate capacity by 22% and deflection increase from 19.5% to 55% respectively .

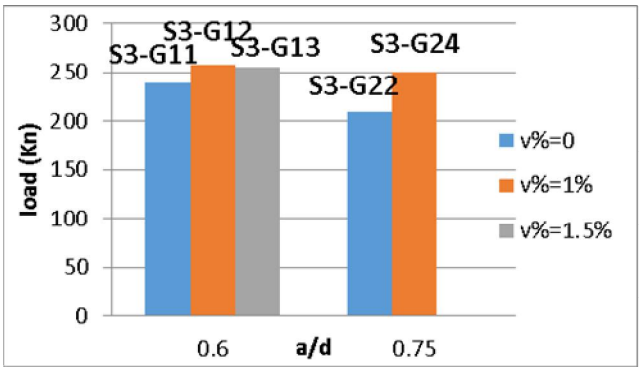

Fig (9)Effect of fiber content on failure load at ultimate load

5.1.2 Effecte shear span to depth ratio a/d

By ANSYS ,It was found that for NSCC corbels, when the (a/d) ratio decreases from 0.6 to 0.45, an increase in cracking load and ultimate load of about 8.8% and 15.4 % is obtained. While when the (a/d) ratio decreases from 0.45 to 0.3, an increase in the cracking load and ultimate load of about 7.1% and 12.7% is achieved. Also, when the (a/d) ratio decreases from 0.6 to 0.3 an increase in the cracking load and ultimate load of about 17.0% and 38.76% is obtained. For HSCC corbels, as the (a/d) ratio decreases from 0.6 to 0.45, an increase in cracking load and ultimate load of about 6.3% and 11.1% is obtained. While when the (a/d) ratio decreases from 0.45 to 0.3, an increase in the cracking load and ultimate load of about 17.9% and 21.69.2% is achieved. Also, when (a/d) ratio decreases from 0.6 to 0.3 the increase in the cracking load and ultimate load of about 25.39% and 35.5% is obtained. This effect is clearly shown from the results listed. By observing the results of the specimens, it is noticed that, with changing the concrete type from NSC to HSC by increasing the compressive strength of concrete from 33.75 to 65.31 MPa, the values of the diagonal crack load increases by 71.0% for specimens with a shear span to effective depth ratio (a/d=0.3) and 53.4% for specimens with a (a/d=0.45) while the specimens that have (a/d=0.6) ,the increase ratio equal to 59.0% as shown in Fig (10) while the Fig (11) shows that increase in shear span-to-depth ratio from 0.45 to 0.6 and 0.75 results in a decrease of 17.61% and 28. % respectively in failure load of corbels without fibers and a decrease of 4% and 7% respectively in failure load of corbels with 1.0% fibers. However, this increase leads to increase of 22% and 23% respectively in deflection at ultimate load of corbels without fibers and increase of 42.3% and 44% respectively in deflection at ultimate load of corbels with 1.0% fibers content.

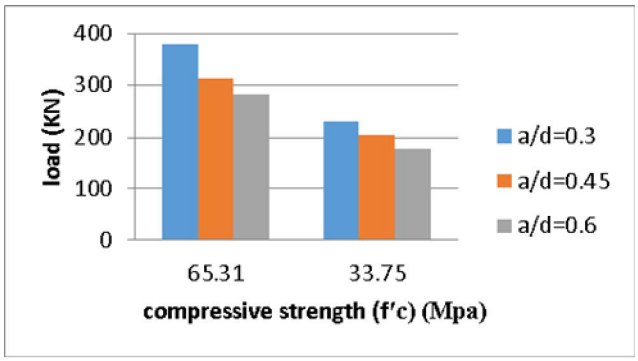

Fig (10): The Effect of Concrete Compressive Strength

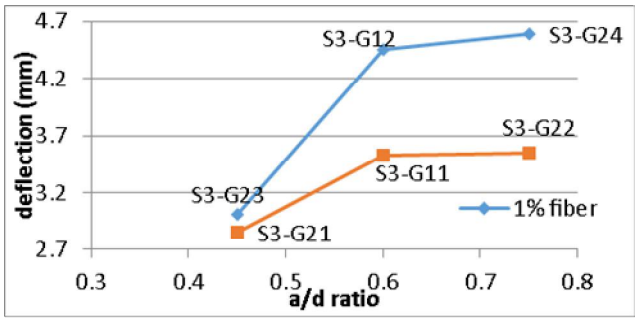

a) Result for deflection

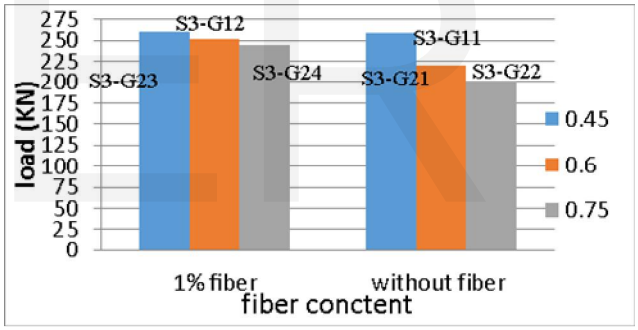

b) Result for ultimate load

Fig (11) Influence of clear depth to overall depth rate on failure force and deflection

5.1.3 Effect of Grade of Concrete

Fig (12) shows that increase in concrete strength from 62.7 N/mm2 to 70.5 N/mm2 and 106.5 N/mm2 results in an increase of 18. % and 23.6% respectively in failure load and a decrease of 6% and 11% respectively in deflection at ultimate load of corbels without fiber. Moreover, increase in concrete strength from 65N/ mm2 to 82N/ mm2 and 106N/ mm2 results in an increase of 25% and 27% respectively in failure load and a decrease of 11.2% and 14% respectively in deflection at 0.9 Pu of corbels with 1.0% fibers content. By ANSYS program it was observed when increasing the concrete compressive strength equal to (40MPa) to (62MPa),for $\rho h.fyh$ values from about 1.535Mpa

and 2.305MPa respectively will increase the ultimate shear strength about 26.0% and 29.5%. Figure(13) observes the influence of compression resistance on maximum share resistance of the experimental corbels.

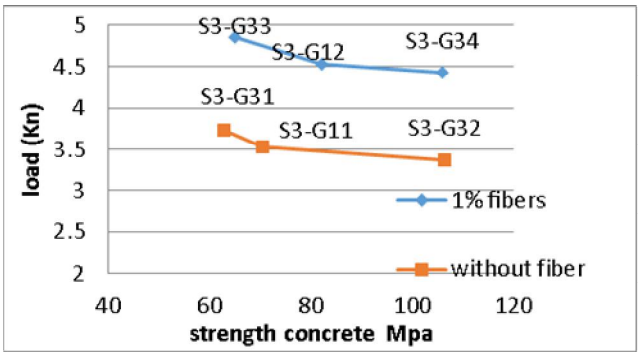

a) Result for deflection

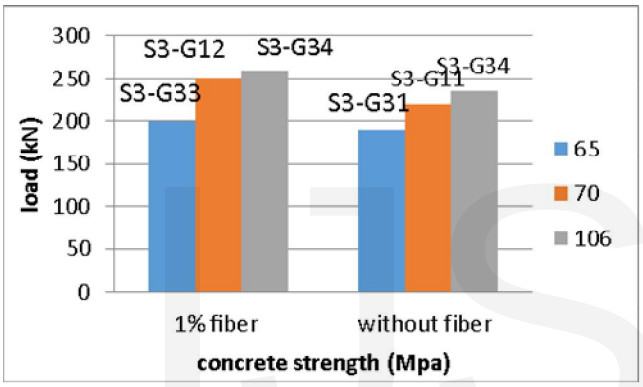

b) Result for ultimate load

Fig (12)Influence of "Concrete strength" on failure force and deflection

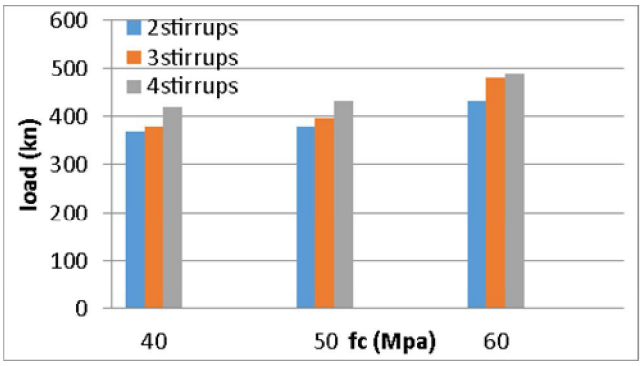

Fig (13) Shear strength versus *fc*'.

5.1.4 Influence of main Reinforcement

The increase in main tension reinforcement by about (100%) led to increase in shear force ability by about (25.5%) with increasing (ρw), the flexural crack has a larger width and length along the column corbel interface when ρw increased for specimens (S2-G52 & S2-G53) as show in Fig (14). It is clear from Fig. (15) shows increase in main steel reinforcement ratio from 1.16% to 2.06% and 2.61% results in an increase of 46.7% and 37.2% respectively in failure load of corbels without fibers and an increase 36% load of corbels with 1.0% fibers content. However, this increase leads to decrease of 4.7% in deflection at ultimate load of corbels without fibers and increase of 16.2 % and 20.73% respectively in deflection at ultimate load of corbels with 1.0% fibers content.

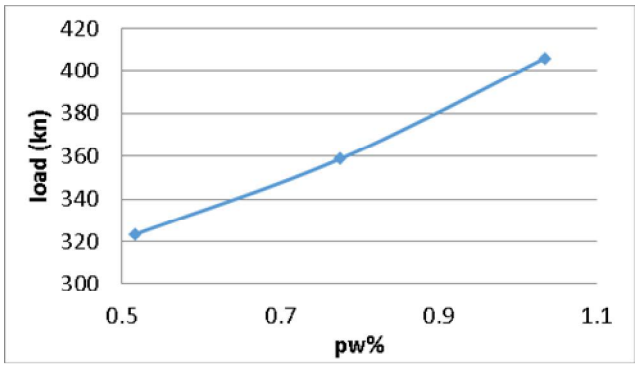

Fig (14) Influence of Main Reinforcement Ratio

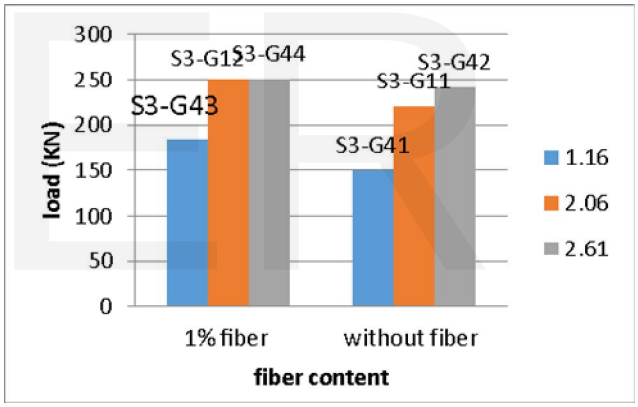

a) Result for ultimate load

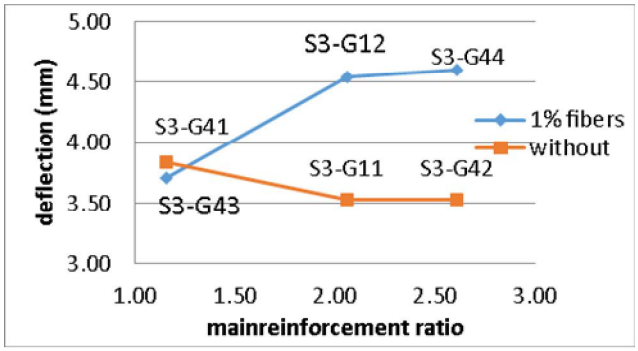

Result for deflection

Fig (15) Influence of Main Reinforcement Ratio on failure load and deflection

5.1.5 Influence of shear reinforcement (stirrup)

An increase in horizontal shear reinforcement index ($\rho h.fyh$) by about 100% caused an increase in ultimate shear strength by about 11.9% and 12.6% for concrete compressive strength equal to about 40 and 50 Mpa respectively, while for concrete compressive strength of 62 MPa, an increase in horizontal shear reinforcement index ($\rho h.fyh$) by about 50% caused an increase in ultimate shear strength by about 14.4% as shown in Fig.(16). This indicates which the contribution of stirrup an increasing ultimate load of the specimen was more effective for specimens with *fc'*=62MPa than specimens having a smallest.

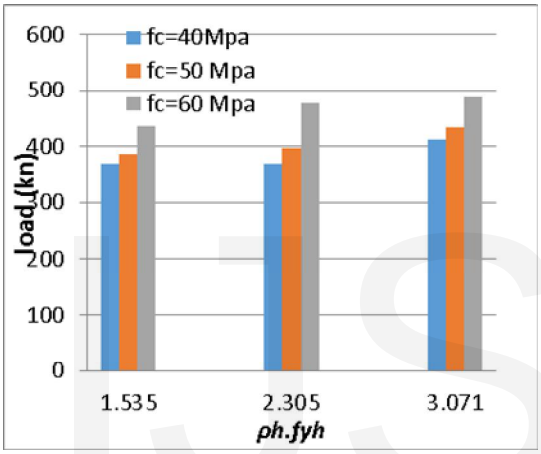

Fig. (16) Shear strength versus

5.1.6 Enfluence of The rate of outside depth to height rate (k/h)

As (*k/h*) increased from 0.24 to 1.00, the ultimate shear strength increased by 12.3%, the effect of (*k/h*) on ultimate shear strength is shown in Figure (4-12). The diagonal tension crack in corbel S2-G51 which has the smallest ratio of *(k/h)* followed a more curved path to the sloping face of the corbel. Truss Model doesn't take the effect of shear reinforcement .

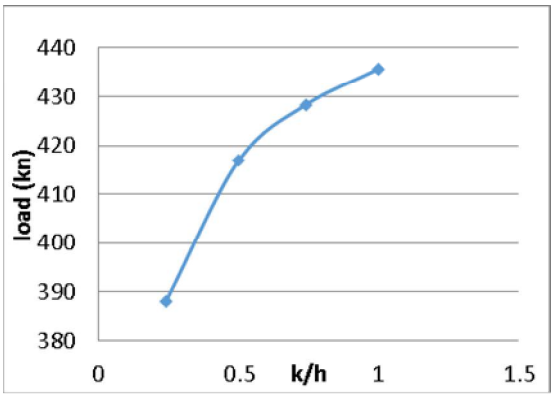

Fig (17) Shear strength versus *k/h*.

5.2 Different Models to Evaluate The Shear Strength of R.C corbels

Many equations were suggested estimate the ultimate, strength of reinforced concrete corbels. Among them, the ACI code [11], Fattuhi equation [12] and Truss method [13]. These equations can briefly presented as follows:

5.2.1 ACI318-14code equation

The ACI- current design produces for corbels were based on shear friction and empirical relationship based on the flexural strength of the segment. The smallest of the five values is used for design. The five basic equations allowed for design of the corbels by ACI318-14 are given as follows:

- shear friction strength

$$v_u = \varphi \mu A_{sm} f_y \quad \text{.....(1)}$$

- Flexural strengt

$$V_u = \frac{M_u}{a} \quad \text{.....(2)}$$

$$M_u = \varphi \rho_w A_f F_y \left(d - \frac{A_f F_y}{1.7 f'_c b}\right) \quad \text{.....(3)}$$

- Maximum shear strength

$$V_u = 0.2 f_c' b d \quad \text{.....(4)}$$

- $V_u = (3.3 + 0.08 f'c) b * d$ .....(5)
- $V_u = 11 b * d$ .....(6)

Where:

V_u = corbel strength (N), $\varnothing$ = strength reduction factor (assumed to be 1.0), μ =coefficient of friction (equal to be1.4for unveils a monolithic unit concrete), A_{sm} = area of reinforcement extending across the critical section (mm^2), As=Area of primary steel , *fy* = yield strength of main reinforcement (N/mm^2), *Mu* = flexural moment (KN.m), a = shear span length (mm), b = width of corbels (mm), *fc'* = cylinder compressive strength (N/mm^2), d = overall depth of corbel (mm).

5.2.2 Fattuhi equation

The predicted values are obtained by using the following modified shear friction equation suggested by Fattuhi

$$v_u = \emptyset\left(\eta A_{vf} f_{fu} \omega\right) + \emptyset\left(A_v f_y \omega\right) \quad \text{.....(7)}$$

Where:

η=overall fiber efficiency factor=0.1, A_{vf}= total area of fibre at critical section (mm^2) calculating by (V%*h*b), f_{fu}=Maximum tensile strength of the fiber (N/mm^2) , $\emptyset$ = strength reduction factor (assumed to be 1.0),

5.2.3Truss Analogy Method (T.A.M)

The equations of the truss analogy method Fig (18) proposed by Hagberg [17], can be listed as follows:

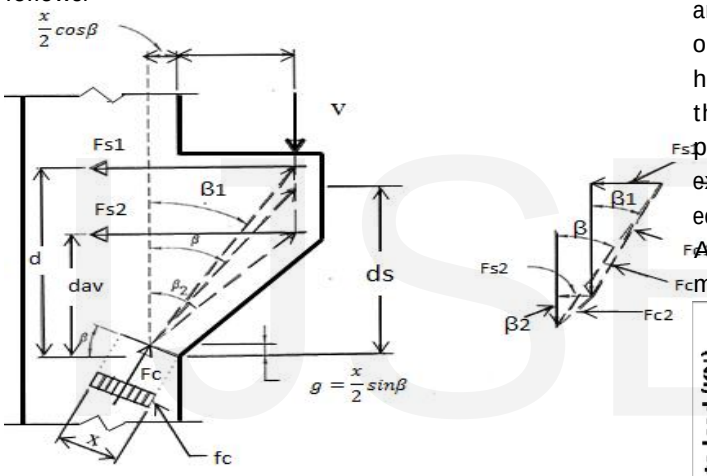

Fig (18) Truss analogy method .

$$\left(1 - \frac{2f'cbd'}{Fs}\right) tan^2\beta + 2\frac{fc}{Fs} tan\beta + 1 = 0 \quad \text{.....(8)}$$

$$ds = d \times \frac{Fst1}{Fs} + dav \times \frac{Fs2}{Fs} \quad \text{.....(9)}$$

$$tan\beta 1 = \frac{a + \frac{x}{2}cos\beta}{d - \frac{x}{2}sin\beta} \quad \text{.....(10)}$$

$$tan\beta 2 = \frac{a + \frac{x}{2}cos\beta}{dav - \frac{x}{2}sin\beta} \quad \text{.....(11)}$$

$$x = \frac{fs}{f'c \cdot b \cdot sin\beta} \quad \text{.....(12)}$$

$$Vu = \frac{Fst1}{tan\beta 1} + \frac{Fst2}{tan\beta 2} \quad \text{.....(13)}$$

Where:

Fs1 = force in main steel (N), *Fs2* = force in stirrups (N), *Fs* = Total force in reinforcements (N), *fy* = yield strength of the main reinforcement (N/mm2), β = angle of inclination of the compressive concrete strut with vertical column Fc=The strut force (compressive strength of concrete)(0.85*f'c*x*b)(KN) x=concrete strut width (mm) ds=The depth of strut force (mm) ,dav=The average depth of center horizontal reinforcement (mm)

The smaller of the two values is used to predicate the ultimate load.

Table 3 and (Fig 19) show a compression between the FEM values of corbels capacity with experimental result and those derived from the above equations. It can be noticed that the Truss angle method is un conservative in NSC while in HSC is conservative except S1-G4 due to lowering the (a/d) and it gave the final numbers which are rather than the ACI-Code equations in assuming the effect of (a/d) values and increasing the (f'c) on the shear strength. While the increasing of the column's width ,we didn't observe any change in ultimate load by FEM and Truss Model when compression the S1-PG5 and S1-PG6 with S1-G1 and S1-G4 respectively in first part from the sires one. Truss model consider the influence of horizontal reinforcement and it doesn't consider the effect of (k/h). The test and numerical protections of corbel forces also these values expected according to ACI318M-14 , fatuhi's equations and truss method, forever the Truss Angle take the increasing in the thickness of the models.

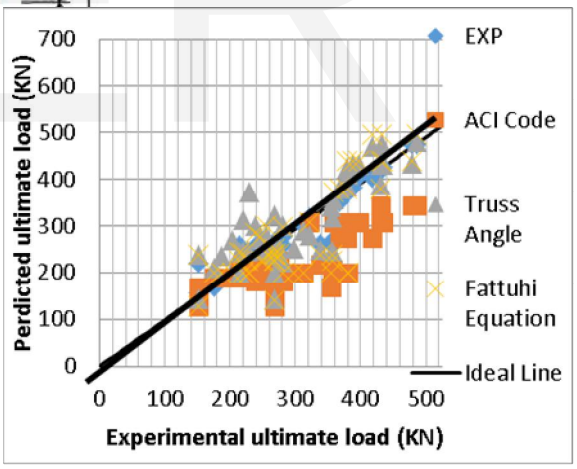

Fig 19-Comprasion between experimental and predicted ultimate loads

6.Conclusions:

Based on the results obtained from the FEM for the reinforced concrete corbels, it concluds that the manner in which shear failure occurs varies widely with dimensions and properties of the corbels. Many factors have significant effect on the shear behavior of corbel at failure, and these effect can be summarized as follows

1- for NSCC corbels, when the a/d ratio lowers from 0.6 to 0.45, have plus in cracking and ultimate loads of about 8.8% and 19.7 %. While when the a/d ratio decreases from 0.45 to 0.3, an increase in the cracking load and ultimate load of about 7.1% and 15.93% respectively is achieved. Also, when the a/d ratio decreased from 0.6 to 0.3 an increase in the cracking and ultimate loads of about 17.9% and 20.2% is obtained.

2- For HSCC corbels, as the a/d ratio decreases from 0.6 to 0.45, an increase in cracking and ultimate loads of about 6.3% and 12.1% has been obtained. While they the a/d ratio decreases from 0.45 to 0.3, an increase in the cracking and ultimate loads of about 17.9% and 20.2% was achieved. Also, when a/d ratio increases from 0.6 to 0.3 the plus in the cracking force and ultimate load is about 25.39% and 35.5%

3- The behaviour of HSC corbel is comparable to which of NSC corbel. The increasing in ($f'c$) causes to rise the force applying strength of the corbels but doesn't led to brittle failure of the corbels.

4- When k/h increase from (0.24) to (1.00), the maximum load increase by 12.3% ,while a plus in stirrup index $\rho h.fyho$ equal to 100 % led to increase in maximum shear resistance which is equal to 11.9% and 12.6% for ($f'c$) is equal to 40Mpa and 50Mpa respectively, while for ($f'c$) of 62MPa, an increase in stirrup index is equal to 50% led to an increase in maximum share resistance is equal to 14.4% ,when increase the primary steel by about (100%) led to increase in shear force ability by about (25.5) with increasing (ρw) .Therefor, growing in steel rate ρw and ρh and k/h causes to increase in corbel stiffness and maximum shear strength.

5- The increasing in horizontal reinforced index $\rho h.fyh$ was more active for specimens with $f'c$=60 MPa than specimens with $f'c$=40 or 50 MPa.

6- The presence of high percentage of fibers or/and horizontal stirrups transformed the mode of failure of the tested corbels into a more ductile one and increased the number of diagonal cracks.

7- Addition of fibre content not only improves the shear strength of the corbels, but also increases the stiffness of these corbels. This improvement is more significant in case of corbels without stirrups.

8- The improvement in shear strength of tested corbels was more significant for specimens with low main reinforcement ratio or these with large shear span-to-depth ratio or those with lower concrete strength.

9- All specimens in series one failed in shear with Diagonal Splitting mode, while in series two, in group one , two, three (except S2-G33), five, and specimen (S2-G42) occurred in Beam Shear the failure was steady. specimen S2-G41 failed in flexural tension. In series three, all corbels failed by the extension of the diagonal crack toward the corbel-column connection. the failure was steady and more ductile than the other specimens that failed in beam shear.

10- Truss Angle method is mostly less conservative when compared with the ACI Code equation, but it gives a good estimate for (a/d) value ,compressive strength concrete ($f'c$) and present or absence shear reinforcement (stirrup) on shear strength.

References

1- ACI Committee 318, 2011, Building Code Requirements for Structural Concrete (ACI 318-14), American Concrete Institute, *Farmington Hills*, USA, pp. 190-194.

2- Rasmussen, L. J., and Baker, G., "Torsion in Reinforced Normal and High-Strength Concrete-Part1 Experimental Test Series", ACI Structural Journal, Jan-Feb. 1995, pp. 56-61.

3- Arnon Bentur & Sidney Mindess, ''Fiber reinforced cementitious composites'' Elsevier applied science London and Newyork 1990.

4- Muhammad, A. H., "Behavior of Strength of High-Strength Fiber Reinforced Concrete Corbels Subjected to Monotonic or Cyclic (Repeated) Loading", Ph.D. Thesis, University of Technology , 1998.

5- ANSYS, Inc., "ANSYS Help", Release 16.1, Documentation,

6- Kasidit Chansawat, Tanarat Potisuk, Thomas H. Miller, Solomon C. Yim, and Damian I. Kachlakev. " FE Models of GFRP and CFRP Strengthening of Reinforced Concrete Beams " . Advances in Civil Engineering Journal , Volume 2009 (2009), pp. 1-13.

7- S. Ahmad, A. Shah, A. Nawaz, K. Salimullah" Shear Strengthening of Corbels with Carbon Fiber Reinforced Polymers (CFRP) " Construction Materials , V. 60, 297, July- September 2010, pp. 79-97.

8- Salman, M., Ihsan Al-Shaarbaf,*Aliewi ,J.,M.,* "Experimental Study on the Behavior of Normal and High Strength Self-compacting Reinforced Concrete Corbels journal of Engineering and Development", Vol. 18, No.6, November 2014, ISSN 1813- 7822

9- Omar and sedeeq, civil "Ultimate Shear strength Of Reinforced High Strength Concrete Corbels Subjected

to Vertical Load" Al-Rafidain Engineering Journal,Vol.18,No.1, Jon.,2010,pp1-12

10- *Hafez ,A., M , Ahmed, M., Diab,H., & Drar ,A., M.,* "Shear HEAR Behavior of of Strength Fiber Reinforced Concrete Corbels" *Journal of Engineering Sciences, Assiut University, Vol. 40, No. 4, pp. 969 -987, July 2012*

11- ACI committee 318. "Building Code Requirement for Reinforcement Concrete (ACI 318-08)," American Concrete Institute, Detroit, 2008.

12- Fattuhi Nijad, "Reinforced Steel Fiber Concrete Corbels with Various Shear Spanto- Depth Ratios", ACI Materials Journal V. 86, No. 6, Nov-Dec 1989.

13- Hagberg, Thore, "Design of Concrete Brackets; On the Application of the Truss Analogy", ACI Journal, Proceedings V. 80, No. 1, January 1983

Table (2). Details of Specimens.

corbel	f'c (Mpa)	dimensions						main reinforcement		secondary reinforcement		a/d	k/h	v%
		a (mm)	d (mm)	h (mm)	b (mm)	c (mm)	Dimensions of column	As	fy	Ahs	fhy			
S1-G1	33.7	69	230	250	150	250	150×200×650	3φ12	420			0.3	0.5	0
S1-G2	33.7	103.5	230	250	150	250	150×200×650	3φ12	420			0.45	0.5	0
S1-G3	33.7	138	230	250	150	250	150×200×650	3φ12	420			0.6	0.5	0
S1-G4	65.31	69	230	250	150	250	150×200×650	3φ12	420			0.3	0.5	0
S1-G5	65.31	103.5	230	250	150	250	150×200×650	3φ12	420			0.45	0.5	0
S1-G6	65.31	138	230	250	150	250	150×200×650	3φ12	420			0.6	0.5	0
S1-PG1	33.75	86.3	230	250	150	250	150×200×651	3φ12	420			0.375	0.5	0
S1-PG2	33.75	121	230	250	150	250	150×200×652	3φ12	420			0.525	0.5	0
S1-PG3	65.75	86.3	230	250	150	250	150×200×653	3φ12	420			0.375	0.5	0
S1-PG4	65.31	121	230	250	150	250	150×200×654	3φ12	420			0.525	0.5	0
S1-PG5	33.75	69	230	250	150	250	150×400×655	3φ12	420			0.3	0.5	0
S1-PG6	65.75	69	230	250	150	250	150×400×656	3φ12	420			0.3	0.5	0
S2-G11	40	133	250	270	180	250	180×200×470	4Φ12	415	2Φ8	415	0.565	0.5	0
S2-G12	50	133	250	270	180	250	180×200×470	4Φ12	415	2Φ8	415	0.565	0.5	0
S2-G13	60	133	250	270	180	250	180×200×470	4Φ12	415	2Φ8	415	0.565	0.5	0
S2-G21	40	133	250	270	180	250	180×200×470	4Φ12	415	3Φ8	415	0.565	0.5	0
S2-G22	50	133	250	270	180	250	180×200×470	4Φ12	415	3Φ8	415	0.565	0.5	0
S2-G23	60	133	250	270	180	250	180×200×470	4Φ12	415	3Φ8	415	0.565	0.5	0
S2-G31	40	133	250	270	180	250	180×200×470	4Φ12	415	4Φ8	415	0.565	0.5	0
S2-G32	50	133	250	270	180	250	180×200×470	4Φ12	415	4Φ8	415	0.565	0.5	0

S2-G33	60	133	250	270	180	250	180×200×470	4Φ12	415	4Φ8	415	0.565	0.5	0
S2-G41	50	133	250	270	180	250	180×200×470	2Φ12	415	3Φ8	415	0.565	0.5	0
S2-G42	50	133	250	270	180	250	180×200×470	3Φ12	415	3Φ8	415	0.565	0.5	0
S2-G51	50	133	250	270	180	250	180×200×470	4Φ12	415	3Φ8	415	0.565	0.24	0
S2-G52	50	133	250	270	180	250	180×200×470	4Φ12	415	3Φ8	415	0.565	0.74	0
S2-G53	50	133	250	270	180	250	180×200×470	4Φ12	415	3Φ8	415	0.565	1	0
S3-G11	70.5	84	140	150	150	200	150*150*550	2φ16	400	----		0.6	1	0
S3-G12	82	84	140	150	150	200	150*150*550	2φ16	400	----		0.6	1	1
S3-G13	75	84	140	150	150	200	150*150*550	2φ16	400	----		0.6	1	1.5
S3-G21	82.4	63	140	150	150	200	150*150*550	2φ16	400	----		0.45	1	0
S3-G22	82.4	105	140	150	150	200	150*150*550	2φ16	400	----		0.75	1	0
S3-G23	96.4	63	140	150	150	200	150*150*550	2φ16	400	----		0.45	1	1
S3-G24	96.4	105	140	150	150	200	150*150*550	2φ16	400	----		0.75	1	1
S3-G31	62.7	84	140	150	150	200	150*150*550	2φ16	400	----		0.6	1	0
S3-G32	106.5	84	140	150	150	200	150*150*550	2φ16	400	----		0.6	1	0
S3-G33	65	84	140	150	150	200	150*150*550	2φ16	400	----		0.6	1	1
S3-G34	106	84	140	150	150	200	150*150*550	2φ16	400	----		0.6	1	1
S3-G41	73	84	140	150	150	200	150*150*550	2φ16	400	----		0.6	1	0
S3-G42	73	84	140	150	150	200	150*150*550	2φ16	400	----		0.6	1	0
S3-G43	94	84	140	150	150	200	150*150*550	2φ16	400	----		0.6	1	1
S3-G44	73	84	140	150	150	200	150*150*550	2φ16	400	----		0.6	1	1
S3-G51	85	84	140	150	150	200	150*150*550	2φ16	400	2φ6	330	0.6	1	0
S3-G52	78.3	84	140	150	150	200	150*150*550	2φ16	400	2φ6	330	0.6	1	1
S3-PG11	70.5	84	140	150	200	200	200*150*550	2φ16	400	-----		0.6	1	0
S3-PG12	82	84	140	150	200	200	200*150*550	2φ16	400	-----		0.6	1	1
S3-PG13	75	84	140	150	200	200	200*150*550	2φ16	400	-----		0.6	1	1.5
S3-PG14	62.7	84	140	150	200	200	200*150*550	2φ16	400	-----		0.6	1	0
S3-PG15	106.5	84	140	150	200	200	200*150*550	2φ16	400	-----		0.6	1	0
S3-PG16	65	84	140	150	200	200	200*150*550	2φ16	400	-----		0.6	1	1
S3-PG17	106	84	140	150	200	200	200*150*550	2φ16	400	-----		0.6	1	1
S3-PG18	70.5	84	140	150	200	200	150*150*550	2φ16	400	-----		0.6	1	0

Table (3): Numerical and test Results

specimen	1st crack load (FEM) (KN)	1st crack load (EXP) (KN)	Ultimate force (Vcr) (KN)					Vcr(EXP)/(Vcr(FEM)
			EXP (P/2)	FEM	ACI	Truss Angle Method	force Fatuhi equation	
S1-G1	68.75	67	217.5	229.7	189.4	372.6		1.056
S1-G2	63.75	63	197.5	203.7	189.4	268.7		1.012
S1-G3	58.75	57.5	169.2	176.5	189.4	208.9		1.02
S1-G4	98.75	98	372.5	380.3	199.4	411		1.02
S1-G5	83.75	81	300	312.5	199.4	289		1.04
S1-G6	78.75	74.5	277.5	281.2	199.4	221.6		1.013
S1-PG1	68.75			220	189	312.7		
S1-PG2	63.75			186.5	189	235.2		
S1-PG3	58.75			355.75	169.3	339.9		
S1-PG4	98.75			298	199.4	250.9		
S1-PG5	68.75			229.75	189	372.6		
S1-PG6	78.75			380.38	199.4	411		
S2-G11	63.7	62.75	350.6	367.5	274.95	378.8		1.05
S2-G12	71.6	65.75	382.8	378.75	308.79	384.2		0.98
S2-G13	83.4	80.75	423.6	431.25	342.63	387.8		1.02
S2-G21	67.7	66.75	373.1	378.75	274.63	423.8		1.02
S2-G22	78.5	77.75	405.8	397.25	308.79	430		0.97
S2-G23	88.3	80.5	475.6	478.75	342.63	434.2		1.01
S2-G31	75	74.125	402	418.25	274.95	468.8		1.04
S2-G32	85.8	84.75	425	431.75	308.79	475.8		1.02
S2-G33	98.1	90.125	475.6	485.75	342.63	480.6		1.02
S2-G41	58.8	55.75	317.8	321.25	306.5	280.3		1.01
S2-G42	69.6	67	350.8	358.75	308.8	356.1		1.02
S2-G51	78.5	77	382.7	388.062	308.8	430		1.01
S2-G52	78.9	76	417.3	430.417	308.8	430		1.03
S2-G53	79.4	75	426.8	433.75	308.8	430		1.02

S3-G11	45	43.125	239	220	187.74	241.2	236	0.920
S3-G12	55	3.4	258	250	207.06	244.6	264	0.969
S3-G13	60	55	260	255	195.3	242.6	277	0.981
S3-G21	45	39.125	268	258.7	207.73	317.2	236	0.965
S3-G22	45	41.75	210	200.7	202.64	198.6	236	0.956
S3-G23	55	50	266	258	225.07	322.2	264	0.970
S3-G24	55	53	250	240	204.34	200.7	264	0.960
S3-G31	45	42	203	190	164.65	238.3	236	0.936
S3-G32	45	38	255	235	217.8	249.4	236	0.921
S3-G33	55	47	220	200	168.3	239.2	264	0.909
S3-G34	55	46	262	255	217.8	249.4	264	0.973
S3-G41	45	38.5	155	150	126.6	142.1	133	0.968
S3-G42	45	42.75	256	241	180.97	298.7	299	0.941
S3-G43	55	53.5	211	184	126.6	143.9	160	0.872
S3-G44	55	48.125	258	257	180.97	298.7	327	0.996
S3-G51	55	53.75	259	230	212.1	271.2	263	0.8881
S3-G52	60	55.75	260	258	200.84	279.9	290	0.992
S3-PG11	45			247	225.2	247.3	225.1	
S3-PG12	55			275.75	225.2	249.9	241.9	
S3-PG13	60			268.75	225.2	248.4	250.3	
S3-PG14	45			227	225.2	245	225.1	
S3-PG15	45			252	225.2	253.8	225.1	
S3-PG16	55			220	225.2	245.7	241.9	
S3-PG17	55			270	225.2	253.7	241.9	
S3-PG18	46			266.35	187.7	241.2	236.7	